*International Journal of Neuropsychopharmacology* (2018) 00(00): 1–11

**doi:10.1093/ijnp/pyy030**
Advance Access Publication: March 15, 2018
Regular Research Article

REGULAR RESEARCH ARTICLE

# Ventral Striatal $D_{2/3}$ Receptor Availability Is Associated with Impulsive Choice Behavior As Well As Limbic Corticostriatal Connectivity

Rebecca L. Barlow, Martin Gorges, Alfie Wearn, Heiko G. Niessen, Jan Kassubek, Jeffrey W. Dalley, Anton Pekcec

Boehringer Ingelheim Pharma GmbH & Co. KG, CNS Discovery Research, Biberach an der Riss, Germany (Dr Barlow, Mr Wearn, and Dr Pekcec); Department of Neurology, University of Ulm, RKU, Ulm, Germany (Drs Gorges and Kassubek); Boehringer Ingelheim Pharma GmbH & Co. KG, Translational Medicine & Clinical Pharmacology, Biberach an der Riss, Germany (Dr Niessen); Department of Psychology, (Dr Dalley), and Department of Psychiatry (Dr Dalley), University of Cambridge, Cambridge, United Kingdom.

Correspondence: Anton Pekcec, DVM, PhD, Boehringer Ingelheim Pharma GmbH & Co. KG, CNS Discovery Research, Birkendorfer Strasse 65, 88397, Biberach an der Riss, Germany (anton.pekcec@boehringer-ingelheim.com).

## Abstract

**Background:** Low dopamine $D_{2/3}$ receptor availability in the nucleus accumbens shell is associated with highly impulsive behavior in rats as measured by premature responses in a cued attentional task. However, it is unclear whether dopamine $D_{2/3}$ receptor availability in the nucleus accumbens is equally linked to intolerance for delayed rewards, a related form of impulsivity.

**Methods:** We investigated the relationship between $D_{2/3}$ receptor availability in the nucleus accumbens and impulsivity in a delay-discounting task where animals must choose between immediate, small-magnitude rewards and delayed, larger-magnitude rewards. Corticostriatal $D_{2/3}$ receptor availability was measured in rats stratified for high and low impulsivity using in vivo [$^{18}$F]fallypride positron emission tomography and ex vivo [$^{3}$H]raclopride autoradiography. Resting-state functional connectivity in limbic corticostriatal networks was also assessed using fMRI.

**Results:** Delay-discounting task impulsivity was inversely related to $D_{2/3}$ receptor availability in the nucleus accumbens core but not the dorsal striatum, with higher $D_{2/3}$ binding in the nucleus accumbens shell of high-impulsive rats compared with low-impulsive rats. $D_{2/3}$ receptor availability was associated with stronger connectivity between the cingulate cortex and hippocampus of high- vs low-impulsive rats.

**Conclusions:** We conclude that delay-discounting task impulsivity is associated with low $D_{2/3}$ receptor binding in the nucleus accumbens core. Thus, two related forms of waiting impulsivity—premature responding and delay intolerance in a delay-of-reward task—implicate an involvement of $D_{2/3}$ receptor availability in the nucleus accumbens shell and core, respectively. This dissociation may be causal or consequential to enhanced functional connectivity of limbic brain circuitry and hold relevance for attention-deficit/hyperactivity disorder, drug addiction, and other psychiatric disorders.

**Keywords:** delay discounting, dopamine $D_{2/3}$ receptor, impulsivity, nucleus accumbens, resting-state fMRI, functional connectivity

**Received:** January 11, 2018; **Revised:** March 8, 2018; **Accepted:** March 14, 2018

## Significance Statement

Understanding the neurobiology underlying choice impulsivity, a psychiatric symptom with cross-diagnostic significance, is key to identifying novel therapies for treating impulsivity. Using the delay discounting task, we selected rats with extreme high- and low-impulsive phenotypes to investigate whether differences in dopamine $D_{2/3}$ receptor binding and functional limbic networks are associated with trait-like impulsivity. We report a novel inverse correlation between $D_{2/3}$ receptor availability in the ventral striatum and impulsive behavior, specifically, lower $D_{2/3}$ receptor binding within the nucleus accumbens core in high- vs low-impulsive rats. Strong connectivity within the limbic network in high- vs low-impulsive rats suggests that differences in striatal $D_{2/3}$ receptor availability may underlie naturally occurring impulsivity and be either causal or consequential to limbic network connectivity modulation.

## Introduction

Impulsivity is a complex, multifaceted behavioral construct, characterized by the tendency to act prematurely and without foresight (Dalley et al., 2011). It can be observed behaviorally as impaired response inhibition ("stopping" impulsivity) or the inability to wait or tolerate delayed rewards ("waiting" impulsivity). Recent progress in the neuroscientific approach to impulsivity has enabled a dissection of these two major components of behavioral function according to their underlying neural substrates (Dalley et al., 2011; Dalley and Robbins, 2017), indicating that overlapping but distinct corticostriatal substrates underlie stopping and waiting subtypes of impulsivity.

Understanding the contribution of inter-individual differences or trait variables to treatment outcome for patients with impulsivity disorders represents a major challenge to the effective treatment of these patients (Dalley et al., 2011). However, investigation into the etiology of natural variation in impulsive choice behavior is limited. Impulsive choice can be defined as the preferential choice of risky or immediate rewards. In addition to "reward discounting," "probability discounting" can be assessed when the dimension of waiting is replaced with that of reinforcer uncertainty. Both forms of discounting behavior contribute to performance on more complex behavioral tasks in a laboratory setting, such as the Iowa Gambling Task (Bechara, 2003) and the delay discounting task (DDT), where a subject's preference for immediate, small rewards vs larger but delayed rewards is assessed.

Deficits in a specific type of impulsive anticipatory responding, often referred to as motor impulsivity or premature responding, have been extensively characterized through numerous neurochemical and neuroanatomical manipulations. Dopamine $D_{2/3}$ receptor availability in the ventral striatum, for example, is predictive of impulsivity on a visual attentional task (Dalley et al., 2007; Besson et al., 2013; Caprioli et al., 2015; Robertson et al., 2015; Dalley and Robbins, 2017).

Imaging studies in normal healthy volunteers as well as patient populations support the link between low striatal $D_{2/3}$ receptor availability, subsequent dopaminergic dysfunction, and elevated levels of self-report and laboratory-assessed impulsivity measures (Lee et al., 2009; Buckholtz et al., 2010; Ghahremani et al., 2012; Ballard et al., 2015). The ventral striatum, including the nucleus accumbens (NAcb), forms part of the limbic system and the orbitofrontal network; changes within these networks may underlie naturally occurring differences in impulsive behavior. Rat lesion studies suggest that the neuroanatomical substrates underlying impulsive choice behavior involve key nodes of these networks, including the NAcb (Cardinal et al., 2001), basolateral amygdala (Winstanley et al., 2004), and hippocampus (Cheung and Cardinal, 2005). Within the prefrontal cortex, the orbitofrontal cortex (OFC) appears to be specifically critical for impulsive choice and consistent with its well-known role in the attribution of reward value and reward-related behaviors (London et al., 2000; Schoenbaum et al., 2009; Rudebeck and Murray, 2014).

In the current study, we investigated whether trait-like impulsivity in the DDT is associated with differences in $D_{2/3}$ receptor binding and corticolimbic functional network modulation. We hypothesized that naturally occurring impulsivity on this task may be associated with low $D_{2/3}$ receptor availability in the ventral striatum, which may impact dopaminergic neurotransmission and functional connectivity within limbic corticostriatal circuitry.

## Materials and Methods

### Subjects and Experimental Design

Subjects were 96 male Lister-hooded rats (Charles River) weighing 250 to 300 g at the start of the experiment and maintained at 85% to 95% of their free-feeding weight. Water was available ad libitum. Animals were group-housed, 4 per cage, and kept under 12-hour-light/-dark cycle (white light on/red light off from 6:00 AM to 6:00 PM). Behavioral experiments were conducted during the day, that is, during the inactive phase of the rats. All experimental procedures were authorized by the Local Animal Care and Use Committee in accordance with local animal care guidelines, Association for Assessment and Accreditation of Laboratory Animal Care regulations and the USDA Animal Welfare Act and took place in an Association for Assessment and Accreditation of Laboratory Animal Care-certified facility. Experiments are reported in accordance with the Animal Research: Reporting of In Vivo Experiments Guidelines (Kilkenny et al., 2012).

We stratified rats according to their behavioral performance on the DDT, selecting those exhibiting extreme high- and low-impulsivity phenotypes, as designated by a number of behavioral measures. Additionally, we screened these rats for variations in baseline locomotor activity to assess the validity and selectivity of the behavior. The selected rats were then assessed for in vivo $D_{2/3}$ receptor availability using [18F]fallypride positron emission tomography (PET) where we focused on cortical as well as dorsal and ventral striatal regions of interest. Ex vivo autoradiography with [3H]raclopride was used to further localize differences in striatal $D_{2/3}$ receptor availability. Although the striatum is an important neural focus of impulsive behavior, it operates within a complex network comprising not only the basal ganglia themselves but also "top-down" influences from limbic structures and the neocortex, including the prefrontal cortex, and "bottom-up" modulation from monoamine systems including, but not limited to, the dopaminergic system (Dalley and Robbins, 2017). The high- and low-impulsive rats were therefore further assessed by fMRI.

### Locomotor Activity

Since impulsivity could be primarily or secondarily affected by differences in motor activity, locomotor activity was assessed using 8 Tru Scan arena chambers each equipped with 2 photobeam sensor rings, allowing the detection of activity in 3 orthogonal planes (Coulbourn Instruments) as previously described (Isherwood et al., 2017). Testing duration was 30 minutes and took place between 1:00 PM and 4:00 PM. Mean distance travelled (cm) over 30 minutes was automatically recorded using Tru Scan 2 software provided by Coulbourn Instruments.

### Delay Discounting

Testing was carried out as previously reported (Isherwood et al., 2017) using 32 operant chambers (Med Associates) enclosed in a sound-attenuating box fitted with a fan for ventilation and masking of external noise. Each chamber was equipped with 2 retractable levers located either side of a centrally located food magazine, into which rodent food pellets (Sandown Scientific) were delivered. A stimulus light was located above each lever, and an infrared beam positioned across the food magazine detected reward collection. The testing apparatus was controlled by Med Associates Software.

Subjects were initially habituated to the test apparatus before commencing lever-press training under a fixed-ratio schedule of reinforcement. During these sessions, both levers were extended and the lever lights were illuminated; a press on either lever resulted in the delivery of a reward pellet. Rats were required to reach a criterion of 60 lever presses within a 60-minute period (30 presses on each lever). After this initial training phase, rats were then exposed to a simplified version of the DDT. Animals were trained to nose-poke in the food magazine to trigger the illumination of a lever light and the presentation of the lever. A response on the lever within 10 seconds (limited hold) resulted in the lever light being extinguished and retraction of the lever, the illumination of the food magazine, and the delivery of a single reward pellet. The levers were presented pseudo-randomly throughout the session. Rats were required to reach a criterion of 60 completed trials within a 60-minute period.

Each training session consisted of 6 blocks of 10 trials, with each trial lasting exactly 72 seconds. Each block of trials began with 4 forced-choice trials, where only one lever was presented in a pseudorandom order. Six free-choice trials were then introduced throughout the task; responding on the right lever resulted in the immediate delivery of a single reward pellet. Responses on the left lever resulted in the delayed delivery of 3 reward pellets, with increasing delay across blocks of 0, 2, 4, 8, 16, and 32 seconds. As in the pretraining protocol, each trial was initiated by the illumination of the house and magazine light. Rats were required to make a nose-poke response in the food magazine within 10 seconds to trigger the presentation of both levers and lever lights. A failure to respond on either lever within 10 seconds (an omission) resulted in the retraction of both levers with all lights extinguished and an inter-trial interval initiated before the next trial. Responding on one of the levers within 10 seconds resulted in the retraction of both levers with all lights extinguished. Reward delivery was preceded by the illumination of the magazine light either immediately or after the chosen delay. The length of the inter-trial interval depended the choice of the immediate or delayed lever and followed reward delivery to ensure each trial was exactly 72 seconds in duration.

### Impulsivity Screening

For stratification rats were ranked, from high to low impulsive, according to their performance on the DDT based on 3 task parameters: the indifference point (the time point at which animals' choice of the delayed lever is 50%), the steepness of the discounting curve (k), and the area under the curve (AUC). The upper and lower 15th centiles of the ranked rats were termed high impulsive (n = 11) and low impulsive (n = 10), respectively (Table 1). The remaining rats were termed mid impulsive (n = 54).

Animals with extreme high and low trait-like impulsivity underwent PET imaging and whole-brain resting-state fMRI and were used for subsequent ex vivo receptor autoradiography studies. The mid impulsive rats were excluded from any further experiments.

### PET Data Acquisition and PET Data Evaluation

All PET scans were performed using the Inveon multi-modality small animal PET/CT scanner (Siemens Healthcare GmbH) with an axial field of view of 12.7 cm and a spatial resolution in the reconstructed images of 1.4 mm (full width at half maximum) (Beltzer et al., 2016). The order of scanning was strictly balanced across days. All data acquisition was carried out under isoflurane anaesthesia (3% for induction and 1.5% for maintenance). For [$^{18}$F]fallypride scans, the animals were placed feet first prone in the central field of view on rat brain beds (Medres). The body temperature of the animals was maintained at 37°C throughout the course of the study using a heating blanket and monitored by a rectal temperature probe. Respiration was monitored by an air-filled pillow positioned under the abdomen of the rats. The breathing frequency was maintained at 75 to 80 cycles/min by adjustment of the anesthesia. [$^{18}$F]fallypride, prepared using a modified method of a previously described radiosynthesis (Mukherjee et al., 1995), was then administered as a bolus (0.5 mL) i.v. via the tail vein with a specific activity of 20.37 ± 3.27 MBq. There were no differences of radioactive-related parameters (injected amounts, specific activity) between the 2 experimental groups. Sixty-minute PET scans were acquired with an energy window of 511 keV and a coincidence window of 3.432

**Table 1.** Mean, Median, and Interquartile Ranges of the Behavioral Measures Used to Assess Impulsivity on the DDT in High- (n = 11), Mid- (n = 54) and Low-Impulsivity (n = 10) Rats

| | AUC | | | k | | | IP | | |
|---|---|---|---|---|---|---|---|---|---|
| | Mean | Median | IQ range | Mean | Median | IQ range | Mean | Median | IQ range |
| HI | 162 | 186 | 48 | 3.421 | 2.096 | 0.533 | 0.347 | 0.404 | 0.139 |
| MI | 872 | 661 | 852 | 0.517 | 0.375 | 0.696 | 5.284 | 2.466 | 5.751 |
| LI | 2659 | 2652 | 807 | 0.014 | 0.011 | 0.021 | 29.31 | 29.31 | 4.620 |

AUC, area under the curve; DDT, delay discounting task; HI, high-impulsivity; IP, indifference point; IQ, interquartile; k, steepness of the discounting curve; LI, low-impulsivity; MI, mid-impulsivity.

ns. PET acquisitions were reconstructed using a filtered back projection algorithm and the following histogramming: 6 × 10 seconds, 3 × 20 seconds, 10 × 60 seconds, 10 × 120 seconds, and 7 × 240 seconds (in total 36 frames). An image zoom of 1 and a 256 × 256 matrix were used yielding in a pixel size of 0.039 cm. An anatomical CT scan was used for attenuation correction. Furthermore, all PET scans were corrected for decay and dead time, and normalization was applied.

[$^{18}$F]fallypride data were analyzed using the simplified reference tissue model (Maier et al., 2014) provided by the Siemens Inveon Research Workplace (version 4.2.0.15) to yield a binding potential. For the determination of binding potential, we used the NAcb, prefrontal cortex, putamen, dorsolateral striatum, and motor cortex as target ROI and the cerebellum as the reference region. This cerebellum reference region was applied to the resliced dynamic [$^{18}$F]fallypride image set to generate a cerebellum time-activity curve. Regions of interest (ROI) were determined using an MRI-based template that was transferred to the PET-CT data set after alignment of MRI and PET brain images.

## Resting-State fMRI Data Acquisition

The high-impulsivity and low-impulsivity subgroups underwent whole-brain resting-state fMRI. Data acquisition was carried out under isoflurane anesthesia (3% for induction and 1.5% for maintenance). The animals were placed in a stereotaxic head support (Bruker BioSpin) to immobilize the head. Body temperature was maintained by an integrated water-based heating at 37°C and monitored by a rectal temperature probe. Respiration was monitored by an air-filled pillow positioned under the abdomen of the rats. The breathing frequency was maintained at 75 to 80 cycles/min by adjusting anesthesia. The rats rapidly recovered after the termination of anesthesia at the end of the MRI procedure. Imaging was done on a 9.4T Biospec scanner (Bruker BioSpin) and acquired with a Bruker linear transmit volume coil and a parallel receive surface array designed for rat's head MRI. First, 3 orthogonal Turbo RARE $T_2$-weighted images were acquired to enable the slice positioning for the fMRI data sets (repetition time [TR] 2000 ms, effective echo time [TE] 20.7 ms, 15 slices, 1 mm). Subsequently, resting-state datasets were acquired using single-shot gradient-echo Echo Planar Imaging (EPI) sequence with TR 2000 ms, TE 20.7 ms. Twelve axial slices of 1 mm and a gap of 0.25 mm were recorded with a field-of-view of 30 × 30 mm$^2$ and matrix size of 128 × 128, resulting in voxel dimensions of 0.23 × 0.23 × 1 mm$^3$. The used bandwidth was 400 kHz (3125 Hz/voxel). Each of the resting-state fMRI data sets comprised 300 repetitions, resulting in a scanning time of 10 minutes for each resting-state fMRI dataset.

## Preprocessing of Functional Imaging Data

To transfer analysis procedures proven valuable in human resting-state fMRI, similar volume-to-voxel size relations as in humans were used for the rat scans. The required voxel resolution and brain grid coverage resulted in a plane (sagittal, coronal) brain grid of approximately 50 voxels and an axial grid of approximately 20 voxels to comparatively match brain grid coverage of standard human resting-state fMRI. Before functional imaging data analysis, to ensure sufficient image quality, all volumes of the EPI images were visually inspected by an experienced neuroimaging expert for proper registration. None of the functional datasets had to be excluded before the analysis because of artifacts. The functional data analysis followed a standardized procedure with adaptation for rodent analysis (Müller et al., 2013) and was performed using the Tensor Imaging and Fiber Tracking software package (Müller et al., 2007). Preprocessing included (1) spatial upsampling to an isogrid, (2) motion correction, (3) normalization, (4) temporal demeaning and linear detrending, (5) temporal bandpass filtering, and (6) spatial smoothing.

Spatial upsampling from 200 × 200 × 750 μm$^3$ into a 55 × 55 × 55 μm$^3$ isogrid (matrix, 256 × 256 × 256) was performed by means of a nonparametric k-nearest neighbor regression approach using the average voxel intensity of the k-nearest neighbor voxels weighted by the inverse of their distance. Upsampling minimizes partial volume effects in mice (Müller et al., 2013). All volumes were motion-corrected using a rigid body transformation in all directions (6 degrees of freedom) with respect to the first volume to correct for physical motion confounding factors such as respiratory and cardiovascular motion as well as potential muscular relaxation of the anesthetized rat body over time. An iterative landmark-based deformation approach was used to normalize all EPI volumes into a standard stereotaxic rat brain (Müller et al., 2013). The functional image time series were demeaned and detrended to correct for possible scanner drifts and were then bandpass filtered using a 6th-order Butterworth bandpass filter design with cut-off frequencies in the range of $0.01 < f < 0.08$ Hz. Spatial filtering was applied to the EPI series by using a 333-μm, 3-dimensional, full-width at half maximum Gaussian blur filter, which equals about twice the in-plane resolution (200 × 200 μm$^2$) as a common choice according to the matched filter design. Finally, the first 30 of the 300 volumes were discarded owing to the transient filter response to correct for possible scanner oscillations at the beginning of the fMRI protocol as well as to allow the rats to adapt to the experimental condition (e.g., noisy environment, muscular relaxation).

## fMRI Data Analysis

Spherical a priori defined seed regions (r = 278 μm) were chosen based on the anatomical structures belonging to the 5 networks of interest to generate the whole-brain correlation maps: (1) a seed in the limbic cortex; (2) a seed in the retrosplenial cortex; (3) a seed in the OFC, and 2 seeds each (4) in the bilateral somatosensory cortex and (5) in the cerebellar cortex were used to generate the whole-brain correlation maps for the (1) limbic network, (2) default mode network, (3) orbitofrontal network (Sforazzini et al., 2014), (4) somatosensory networks (Jonckers et al., 2011), and (5) cerebellar network, respectively (Sforazzini et al., 2014). The seed regions used to define the networks are common choices, since the seeds are located in major nodes of the corresponding functional networks (Smith et al., 2009; Laird et al., 2011). The extracted arithmetically averaged time-courses of each seed region were correlated with the time series of all other voxels across the whole brain, yielding a corresponding Pearson's product moment correlation coefficient ($r$-value) for each voxel. Finally, the individual animal's correlation maps were Fisher's $r$- to $z$-transformed to normally distributed $z(r)$ scores that were used for statistical analysis.

The two-sided parametric Student's $t$ test for unequal variances was used to test for voxel-wise differences between low- and high-impulsivity rats for both networks. Possible correlations between functional connectivity measures and impulsivity were studied using a data-driven approach by means of Spearman rank-order correlation (Gorges et al., 2016). The $z(r)$ scores corresponding to the limbic and orbitofrontal networks were correlated with the DDT–AUC score for each voxel across the whole brain for each network. The resulting $P$ values for

(1) group comparison and (2) correlation analysis were considered as statistically significant at $P<.05$ and corrected for multiple comparisons using the false discovery rate (FDR) approach (Genovese et al., 2002) at a 5% level. Further cluster-wise correction for multiple comparisons was performed by a parametric correlation-based clustering procedure that discarded isolated clusters not exceeding the minimum size of 343 voxels in the isogrid, that is, ≤0.057 $mm^3$.

### Ex Vivo Receptor Autoradiography

Subjects were killed by overdose of pentobarbital and cervical dislocation. Brains were rapidly removed and placed on a steel dissection plate, cooled on dry ice, with the dorsal surface uppermost before being frozen at –80°C. Brains were sectioned in the coronal plane using a Jung CM300 cryostat (Leica). For autoradiography, consecutive 20-µm slices throughout the striatum were mounted on Superfrost Plus microscope slides (Fisher Scientific). Sections were stored at –80°C before being thawed at room temperature for processing.

[$^3$H]Raclopride (2812 GBq/mmol) was purchased from PerkinElmer. Haloperidol was purchased from Sigma-Aldrich. Duplicate, consecutive slides were prewashed for 15 minutes at room temperature in 120 mM of Tris-HCl (pH 7.4). Slides were incubated in a buffer containing 10 nM of the radioligand for 1 hour. For nonspecific binding, additional 10 µM of cold ligand was added to the incubation buffer. Following incubation, slides were washed twice in fresh 4°C buffer for 2 minutes and then rinsed in distilled-deionized water. Slides were air-dried for at least 2 hours before being fixed in 4% PFA. These were subsequently apposed with tritium microscale standards (Amersham Biosciences) to a tritium-sensitive phosphor-imaging plate (Fujifilm). The plates were scanned using a FLA-5000 Bio-Imaging Analyzer (Fujifilm) to digitize autoradiographs at 16-bit grey scale for image analysis. ROI analysis was conducted using ImageJ (Abramoff M, 2004).

### Statistical Analysis

Behavioral and PET imaging data were analyzed using Statistica 12 (Dell Statistica) and GraphPad Prism 6 (GraphPad Software). Locomotor activity data were expressed as the distance travelled over the test period of 30 minutes. Data were analyzed using a nonpaired, two-tailed Student's *t* test. Repeated-measures ANOVA with a between-subjects factor was used to compare [$^{18}$F]fallypride and [$^{3H}$]raclopride binding in high- and low-impulsivity groups. Where significant main effects were found, posthoc analysis using Fisher's least significant difference (LSD) test was performed. When the assumption of homogeneity of variance could not be met, a Games–Howell test was used. Statistical significance was set at $\alpha=0.05$. Analysis of the functional imaging data is detailed above. All data are given as mean ± SEM.

## Results

### Behavioral Screening

Rats that completed training on the DDT (average >85% choice of the large-reward lever at a 0-second delay over last 6 days; n = 75) were segregated into 3 groups according to their performance. Figure 1 shows the discounting curves for high- and low-impulsive rats in relation to the rest of the cohort (mid-impulsive rats). Descriptive statistics of the 3 behavioral measures in high- (n = 11), mid- (n = 54), and low-impulsive (n = 10) rats are detailed in Table 1. One-Way ANOVA revealed a significant difference between the 3 impulsivity groups with regards to the AUC ($F(2,72)=66.48$, $P<.001$), k ($F(2,72)=28.11$, $P<.001$), and the IP ($F(2,72)=24.49$, $P<.001$). Posthoc analysis using Fisher's LSD test is detailed in Table 2. Analysis of locomotor activity in a novel environment revealed no significant difference in baseline locomotor activity between high- and low-impulsive rats ($t(20)=1.68$, $P>.05$) (Table 3).

### Low $D_{2/3}$ Receptor Availability Is Associated with Increased DDT Impulsivity

Although no significant differences between high- and low-impulsive rats were observed in $D_{2/3}$ receptor availability in the prefrontal cortex ($F(1,19)=0.03$, $P>.05$), dorsal striatum ($F(1,19)=0.23$, $P>.05$), or NAcb ($F(1,19)=0.89$, $P>.05$; Figure 2), a significant correlation was observed between the binding potential of [$^{18}$F]fallypride in the left NAcb and both the AUC ($r_s=-0.78$, $P<.01$) and IP ($r_s=-0.79$, $P<.01$) (Figure 2). No such association was observed in low-impulsive rats.

### Low $D_2$ Receptor Availability Is Localized to the Core Subregion of the NAcb

Analysis of $D_2$ receptor binding using [$^3$H]raclopride autoradiography revealed a lower $D_2$ receptor availability in the left NAcb core region of high-impulsive rats vs low-impulsive rats ($F(1,19)=6.69$, $P<.05$) accompanied by relative higher $D_{2/3}$ receptor availability in both the left and right NAcb shell ($F(1,19)=6.13$, $P<.05$; Figure 3). No significant differences in $D_2$ binding were observed in either the dorsomedial or dorsolateral striatum. Additionally, a dimensional relationship between DDT impulsivity and $D_{2/3}$ receptor availability in the left NAcb shell was observed, specifically in low-impulsive rats where low impulsivity, as measured by the AUC, was associated with high $D_{2/3}$ receptor availability ($r_s=-0.63$, $P<.01$; Figure 3).

### Increased Functional Brain Connectivity Is Associated with High Impulsive Behavior

The correlation between $D_{2/3}$ receptor availability in the left NAcb and high trait-like impulsivity suggested a potential modulation of functional connectivity in limbic brain circuitry. To quantify limbic functional connectivity, we measured BOLD coherence for the limbic network using a seed region in the cingulate cortex and demonstrated a consistent functional brain connectivity

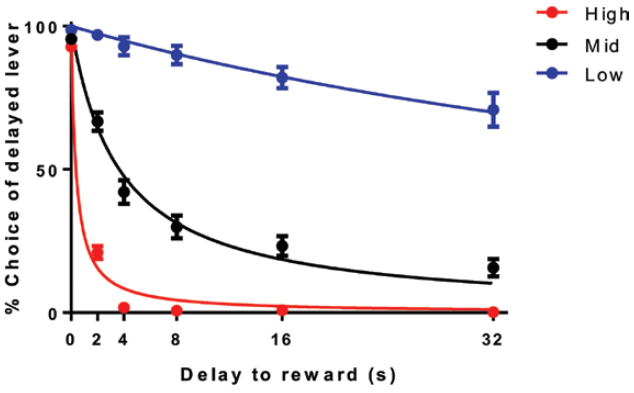


**Figure 1.** Delay discounting curves for high- (n = 11), mid- (n = 54), and low-impulsive (n = 10) rats. Data presented as mean ± SEM.

**Table 2.** Summary of Posthoc Fisher's LSD Test, Assessing Differences in AUC, k, and IP between High- (n = 11), Mid- (n = 54), and Low-Impulsivity (n = 10) Rats

| | AUC | | | k | | | IP | | |
|---|---|---|---|---|---|---|---|---|---|
| | HI | MI | LI | HI | MI | LI | HI | MI | LI |
| HI | | <0.001 | <0.001 | | <0.001 | <0.001 | | <0.01 | <0.001 |
| MI | <0.001 | | <0.001 | <0.001 | | NS | <0.01 | | <0.001 |
| LI | <0.001 | <0.001 | | <0.001 | NS | | <0.001 | <0.001 | |

AUC, area under the curve; HI, high-impulsivity; IP, indifference point; IQ, interquartile; k, steepness of the discounting curve; LI, low-impulsivity; LSD, least significant difference; MI, mid-impulsivity.

**Table 3.** Different Measures of Spontaneous Activity Do Not Differ between Rats Selected for High- and Low-Impulsive Phenotype

| Behavior Measured | Low-Impulsive Rats | High-Impulsive Rats | Statistics |
|---|---|---|---|
| Average distance moved (cm) | 5207 ± 142 | 4876 ± 209 | ns |
| Average rearing frequency (total number) | 135 ± 6 | 123 ± 7 | ns |
| Rearing time (average) (s) | 372 ± 24 | 335 ± 27 | ns |

Comparison of activity-dependent parameters between the high- and low-impulsivity subgroups of rats was assessed using a two-tailed unpaired Student's t test. Statistical significance for all tests was set to $P < .05$; ns, lack of statistical significance, i.e., $P > .05$. Data are given as mean ± SEM.

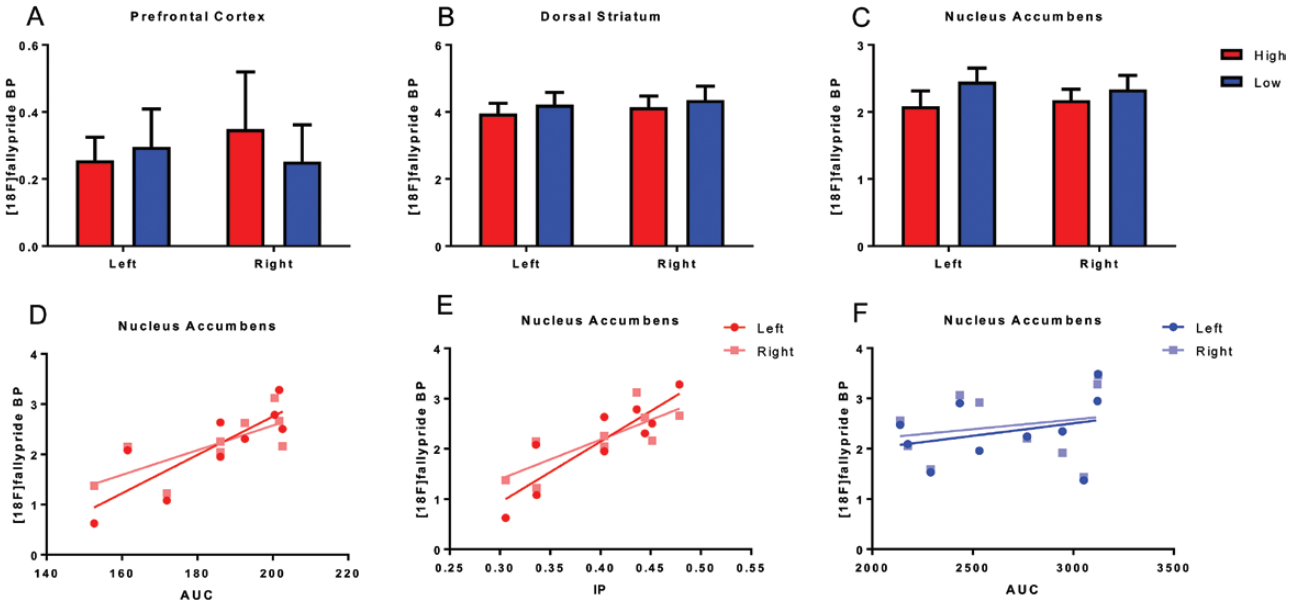


**Figure 2.** [$^{18}$F]fallypride binding potential (BP) in the left and right hemispheres of the (A) prefrontal cortex, (B) dorsal striatum, and (C) nucleus accumbens (NAcb) of high- (n = 11) and low-impulsive (n = 10) rats. Data presented as mean ± SEM. Correlations between area under the curve (AUC) and indifference point (IP) scores in the left and right hemispheres of high- (D–E) and low-impulsive (E) rats in the NAcb.

map of the limbic system for both low- and high-impulsivity rats (Figure 4A) in agreement with other groups (Müller et al., 2007). Comparison across the whole brain between low- and high-impulsive rats (unpaired $t < -2.5$; $P < .05$, FDR corrected for multiple comparisons) indicated significantly stronger BOLD synchronization within the limbic network, that is, higher functional connectivity, in high- vs low-impulsive rats. Particularly marked effects were observed bilaterally for the hippocampal formation, indicating significant functional coupling with the cingulate cortex in high-impulsive rats. Less-marked effects were seen in the striatum, with stronger functional connectivity with the cingulate cortex in high-impulsive rats (Figure 4A).

We then assessed functional connectivity in the orbitofrontal network, because DDT impulsivity is associated with dopaminergic signaling in the OFC (Zeeb et al., 2010); the functional connectivity networks revealed similar BOLD synchronization in high- and low-impulsive rats (Figure 4C) as indicated by voxel-wise group comparison ($P > .05$). By contrast, correlation analysis indicated significant positive correlations between regional orbitofrontal functional network connectivity and the DDT-AUC impulsivity score ($r > 0.5$; $P < .05$, FDR corrected). As shown in Figure 4D, bilateral functional connectivity of the hippocampal formation was also significantly correlated with the DDT-AUC score, that is, the greater the functional coupling between the hippocampal formation and the OFC, the higher the DDT impulsivity. In summary, higher DDT-AUC scores were correlated with regional functional connectivity in limbic and orbitofrontal networks, confirming that these are associated with this measure. However, only high-impulsive rats showed significantly enhanced connectivity in limbic but not in orbitofrontal networks.

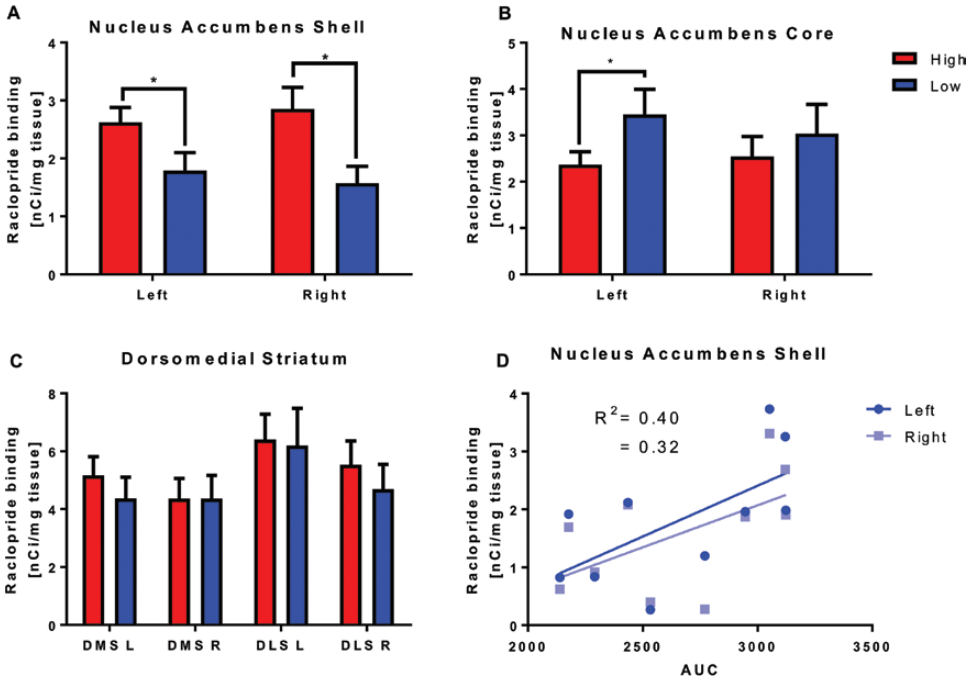


**Figure 3.** [$^3$H]raclopride binding (nCi/mg tissue) in the left and right hemispheres of the (A) nucleus accumbens (NAcb) shell, (B) NAcb core, and (C) dorsal striatum (DMS, dorsomedial striatum; DLS, dorsolateral striatum) of high- (n = 11) and low-impulsive (n = 10) rats. Data presented as mean ± SEM. (D) Correlations between area under the curve (AUC) in the left and right hemispheres the NAcb shell of low-impulsivity rats. *$P < .05$.

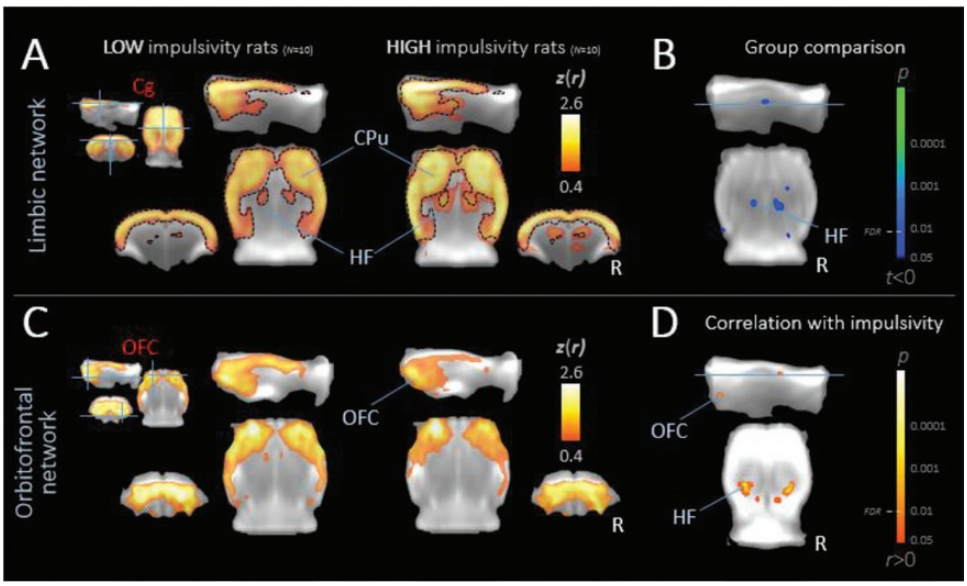


**Figure 4.** Intrinsic functional connectivity maps in low- (left column) and high-impulsive rats (right column) and its correlations with impulsivity. (A, C) Blood oxygenation level–dependent (BOLD) synchronization illustrated as connectivity heat maps showing voxel-wise Fisher's *r*-to-*z* transformed Pearson's correlation coefficients (thresholded for $|z(r)| \geq 0.4$) for which the fMRI BOLD signal was correlated with the signal in the limbic network (Cg, cingulate gyrus, A) and the orbitofrontal network (orbitofrontal cortex [OFC], C). Color coded *z*(*r*)-values indicate the strength of correlation for each voxel with respect to the seed region as a measure of functional connectivity. (B) Statistical group comparison (cool colors; corrected $P < .05$ for multiple comparisons in voxel-wise Student's *t* tests) for the limbic network indicated significantly enhanced functional connectivity in high-impulsive rats (n = 11) compared with low-impulsive (n = 10) rats. These patterns of strong functional connectivity presented as an enlarged limbic network as illustrated by the delineations (black solid lines, A) corresponding to the limbic functional connectivity network in the low-impulsivity rats (B, left). (C) The orbitofrontal network demonstrated similar functional connectivity maps for low- (left) and high-impulsive rats (right); statistical analysis (voxel-wise Student's t tests) revealed no significant differences between groups. (D) Significantly positive correlations (hot colors; corrected $P < .05$; voxel-wise Spearman rank order correlations) were demonstrated for orbitofrontal network connectivity with the impulsive choice score (area under the curve [AUC]) represented as orthogonal pair of slices in all rats. Clusters indicating statistically significant group effects or significant correlations with the impulsive choice score (AUC) were corrected at a 5% false discovery rate (FDR)-level with further cluster-wise correction (minimum size 0.057 mm$^3$). All results are shown in stereotaxic space (55 μm isogrid) overlaid on the averaged study-specific Echo Planar Imaging (EPI) template (n = 20). CPu, caudate and putamen; HF, hippocampal formation, R, right.

## Discussion

Our findings support our hypothesis that low $D_{2/3}$ receptor availability and functional connectivity modulations within limbic corticostriatal circuitry are associated with increased preference for immediate small-magnitude rewards (i.e., delay aversion). We thus extend earlier reports of low $D_{2/3}$ receptor availability in the ventral striatum and specifically the NAcb shell in a related form of waiting impulsivity (Dalley et al., 2007; Besson et al., 2010). Our findings indicate that increased delay aversion in the DDT is inversely associated with low $D_{2/3}$ receptor availability in the NAcb core. Thus, different forms of waiting impulsivity involving an inability to suppress premature responding when rewards are delayed or when rewards are subjectively devalued over time both associate with low $D_{2/3}$ receptor availability but in different subregions of the NAcb.

Rats selected for extreme low and high impulsivity on the 5-choice serial reaction time task exhibit differential $D_{2/3}$ receptor availabilities in the ventral striatum, as measured using [$^{18}$F]fallypride-PET (Dalley et al., 2007). In this study, a significant inverse correlation between $D_{2/3}$ receptor availability in the ventral but not dorsal striatum and premature responses (a measure of impulsivity) was observed. High-impulsive animals on this task maintained significantly higher rates of cocaine self-administration than low-impulsive rats (Dalley et al., 2007) and subsequently developed compulsive cocaine self-administration (Belin et al., 2008). Similarly, high- and low-impulsive rats selected on the DDT demonstrated that impulsive choice predicts resistance to extinction and a propensity to relapse to cocaine seeking (Broos et al., 2012).

A plethora of human imaging studies indicate reduced striatal availability of $D_2$-like dopamine receptors in patients with stimulant-use disorder and other addiction pathologies, which might already partially exist before drug exposure and may predispose for addictive behaviors (for review see, Ashok et al., 2017). Since self-report impulsivity is negatively correlated with $D_{2/3}$ availability in the ventral striatum and globus pallidus (Buckholtz et al., 2010; Caravaggio et al., 2016) and high trait-like impulsivity is a predisposing factor for substance abuse (Robbins et al., 2012), these studies highlight a potential overlap of $D_2$-like dopamine receptors with both impulsivity and substance abuse vulnerability. As per the original observation, we observed a significant inverse correlation between $D_{2/3}$ receptor availability and choice impulsivity in the ventral, but not dorsal striatum by [$^{18}$F]fallypride PET imaging, specifically in high-impulsive rats. This suggests a common neurobiological substrate underlying both impulsive choice as assessed on the DDT and motor impulsivity as assessed on the 5-choice serial reaction time task. Ex vivo receptor autoradiography analysis demonstrated that high-impulsive rats exhibited significantly lower $D_2$ receptor binding within the NAcb core vs low-impulsive rats associated with a concurrent higher $D_2$ receptor binding in the NAcb shell subregion, significant in the left hemisphere only. Taken together, these data point to a dysfunction of striatal dopaminergic neurotransmission, in line with a recent report demonstrating altered dopamine release in the NAcb core of high- vs low-impulsive rats selected on the DDT (Moschak and Carelli, 2017).

Recent clinical studies link alterations in striatal $D_{2/3}$ receptor availability and subsequent dopaminergic dysfunction with attention deficit hyperactivity disorder (ADHD), a condition characterized by both motor (Lipszyc and Schachar, 2010) and choice impulsivity (Patros et al., 2016). PET studies in adult medication-naive ADHD patients found reduced $D_{2/3}$ receptor availability in the NAcb and caudate (Volkow et al., 2009). Treatment response to stimulants is associated with increased dopamine transmission in the ventral striatum (Volkow et al., 2012; Caprioli et al., 2015), indicating that the efficacy of ADHD medication may depend, in part, on restoring $D_{2/3}$ receptor signaling of impulsive individuals. Substance abusers and obese individuals with and without binge eating disorder also have decreased $D_{2/3}$ receptor availability in the striatum, which can manifest as a tendency for natural rewards to lose their value (Volkow et al., 2008) as well as enhanced impulsivity (Dawe and Loxton, 2004; Nederkoorn et al., 2006; Galanti et al., 2007). Such impairments can present as discounting deficits, where immediate smaller rewards hold greater salience than larger future gains due to an impaired reinforcement system (Wang et al., 2004; Volkow et al., 2008) resulting in a tendency towards impulsive responding (Robbins et al., 2012). In accordance with this hypothesis, a recent imaging study in patients with substance use disorder found a negative correlation between striatal $D_{2/3}$ receptor availability with preference for smaller, more immediate rewards over larger, delayed alternatives (Ballard et al., 2015). Interestingly, a computational modeling approach aiming to determine the functional role of ventral striatal dopamine $D_2$-receptor in the expression of previously acquired behaviors predicted this finding and suggests that dopamine $D_2$-receptor manipulation in the ventral striatum selectively modulates motivated behavior for distal vs proximal outcomes. Specifically, the model quantitatively accounts the steepness of discounting on a DDT as a function of $D_2$-dependent tonic dopamine firing in the ventral striatum (Smith et al., 2005).

Dysfunction of midbrain dopaminergic systems have been implicated in several forms of impulsive behavior in rodents, especially within the NAcb (Dalley et al., 2007; Besson et al., 2010; Dalley and Robbins, 2017). NAcb core lesions shift behavior toward the choice of small, immediate food rewards, although damage to 2 of its afferents, the anterior cingulate cortex and medial prefrontal cortex, is without effect (Cardinal et al., 2001; Pothuizen et al., 2005; Basar et al., 2010) and there is evidence the NAcb core is also important for modulating probability discounting (Basar et al., 2010). The NAcb is part of a larger network encompassing the amygdala and prefrontal cortex. As such, lesions on the basolateral amygdala and OFC exert qualitatively similar effects on impulsive choice as those on the NAcb core (Mobini et al., 2002; Winstanley et al., 2004; Rudebeck et al., 2006). However, the opposite preference for a larger delayed reward has also been reported with regard to OFC lesions, potentially owing to variations in task procedure, such as inclusion of a conditioned reinforcer during the delay interval (Winstanley et al., 2004; Zeeb et al., 2010). The importance of the OFC in regulating impulsive choice has been established through observations of enhanced dopamine release during the choice phase of DDT and by molecular changes, induced by impulsive behavior itself within the OFC (Zeeb et al., 2010). An association between changes in the activation of limbic frontostriatal networks with age-dependent reductions in impulsive choice have previously been reported in a human temporal discounting task (Christakou et al., 2011), suggesting that altered activation coupling between areas such as the anterior cingulate cortex, OFC, striatum, and amygdala may underlie naturally occurring impulsive choice behavior.

Our resting-state functional connectivity data are consistent with previous findings in humans (Davis et al., 2013; Gorges et al., 2015, 2016) and rodents (Power et al., 2012; Zhan et al., 2014), demonstrating that abnormal functional integration of specific disease-related networks is associated with different behavioral phenotypes. Specifically, rats selected for extreme

impulsivity phenotypes exhibited a pattern of increased functional connectivity within the major limbic system nodes. These findings were strengthened by abnormally increased region-to-region connectivity within the limbic network of high-impulsivity rats, similar to that shown in patients with ADHD, especially hyperactive-impulsive subtypes (Sanefuji et al., 2017).

Orbitofrontal network connectivity did not differ between high- and low-impulsive rats, although it correlated with choice impulsivity as measured by numerous behavioral scores. Within this network, low NAcb core $D_{2/3}$ receptor availability may result in an imbalanced dopaminergic-mediated functional coupling that may underlie naturally occurring choice impulsivity. Imaging studies in ADHD report increased connectivity between the NAcb core and prefrontal cortex associated with increased choice impulsivity (Costa Dias et al., 2013), as well as atypical activation of the NAcb and OFC when performing the DDT (Plichta et al., 2009). In line with this, methamphetamine users exhibit low striatal $D_{2/3}$ receptor availability and poor inhibitory control and choice impulsivity. Thus, impaired activation and connectivity in frontostriatal networks may underlie aberrant reward-driven behavior in methamphetamine users (Kohno et al., 2014; London et al., 2015). Since reduced striatal $D_{2/3}$ receptor availability has been shown in ADHD and methamphetamine users (Volkow et al., 2009; Kohno et al., 2014), alterations in OFC activation and orbitofrontal network connectivity may be secondary and consequential to altered striatal dopaminergic neurotransmission. In Parkinson's disease, ongoing dopaminergic cell degeneration is associated with increased functional connectivity early in the disease (Gorges et al., 2015). Therefore, any imbalance in the dopaminergic system associated with abnormal functional coupling could potentially result in altered behavioral performance, specifically neurobiological changes in the limbic system including the NAcb. A caveat is that functional connectivity results can be only indirectly assessed from the limited signal-to-noise ratio of the BOLD signal acquired at a given spatial resolution (Power et al., 2012).

Resting-state fMRI is an indirect measure for functional connectivity constrained by the limited signal-to-noise ratio and limited spatial resolution (Gorges et al., 2017). The seed-based approach measures connectivity with respect to the reference voxel and, hence, does not characterize the full functional connectome, which presents a limitation of the current study. Future studies might utilize connectome-based approaches that model the NAcb together with relevant regions of the limbic system as nodes. In addition, we cannot exclude the possibility that general anesthesia influenced resting-state functional connectivity presenting a potential limitation of our study. A further caveat is that of [$^{18}$F]fallypride lacks selectivity for $D_2$ over $D_3$ receptors(Mukherjee et al., 2002). Further studies with more selective PET tracers are thus needed to resolve the relative involvement of $D_2$ and $D_3$ receptors in choice impulsivity.

In summary, we report a significant correlation between low $D_{2/3}$ receptor availability in the ventral striatum and increased DDT impulsivity, specifically, lower $D_{2/3}$ receptor binding within the NAcb core of high- vs low-impulsive rats. The strong connectivity within the limbic network in high- vs low-impulsive rats supports the hypothesis that differences in $D_{2/3}$ receptor binding within the NAcb may underlie naturally occurring variation in waiting impulsivity and be either causal or consequential to modulations of limbic network connectivity. An important question for future research is whether interventions that increase striatal $D_{2/3}$ receptor availability can normalize high impulsivity and attenuate associated limbic hyper-connectivity. Understanding the neurobiological processes underlying waiting impulsivity is key to identifying novel treatment strategies for treating impulsivity as a specific psychiatric symptom with cross-diagnostic significance (Dalley and Robbins, 2017).

## Funding

This work was supported in full by Boehringer Ingelheim Pharma GmbH & Co. KG, Div. Research Germany, Birkendorf Strasse 65, 88397, Biberach an der Riss, Germany.

## Acknowledgments

We thank Andrea Vögtle, Thomas Kaulisch, Peter Schorn, and David Kind for excellent technical support and Detlef Stiller and Janet Nicholson for helpful scientific discussion. Editorial support and formatting assistance for this manuscript were provided by Michelle Marvel, BA, and Heather Shawcross, PhD, of Fishawack Communications Ltd, funded by Boehringer Ingelheim.

## Statement of Interest

R.L.B., A.W., H.G.N., and A.P. are employees of Boehringer Ingelheim Pharma GmbH & Co. K.G. M.G., J.K., and J.W.D. declare no conflicts of interest.

## References

Abramoff MD, Magalhães PJ, Ram SJ (2004) Image processing with ImageJ. Biophotonics Int 11:36–42.

Ashok AH, Mizuno Y, Volkow ND, Howes OD (2017) Association of stimulant use with dopaminergic alterations in users of cocaine, amphetamine, or methamphetamine: a systematic review and meta-analysis. JAMA Psychiatry 74:511–519.

Ballard ME, Mandelkern MA, Monterosso JR, Hsu E, Robertson CL, Ishibashi K, Dean AC, London ED (2015) Low dopamine D2/D3 receptor availability is associated with steep discounting of delayed rewards in methamphetamine dependence. Int J Neuropsychopharmacol 18:pyu119.

Basar K, Sesia T, Groenewegen H, Steinbusch HW, Visser-Vandewalle V, Temel Y (2010) Nucleus accumbens and impulsivity. Prog Neurobiol 92:533–557.

Bechara A (2003) Risky business: emotion, decision-making, and addiction. J Gambl Stud 19:23–51.

Belin D, Mar AC, Dalley JW, Robbins TW, Everitt BJ (2008) High impulsivity predicts the switch to compulsive cocaine-taking. Science 320:1352–1355.

Beltzer A, Kaulisch T, Bluhmki T, Schoenberger T, Stierstorfer B, Stiller D (2016) Evaluation of quantitative imaging biomarkers in the DSS colitis model. Mol Imaging Biol 18:697–704.

Besson M, Belin D, McNamara R, Theobald DE, Castel A, Beckett VL, Crittenden BM, Newman AH, Everitt BJ, Robbins TW, Dalley JW (2010) Dissociable control of impulsivity in rats by dopamine d2/3 receptors in the core and shell subregions of the nucleus accumbens. Neuropsychopharmacology 35:560–569.

Besson M, Pelloux Y, Dilleen R, Theobald DE, Lyon A, Belin-Rauscent A, Robbins TW, Dalley JW, Everitt BJ, Belin D (2013) Cocaine modulation of frontostriatal expression of zif268, D2, and 5-HT2C receptors in high and low impulsive rats. Neuropsychopharmacology 38:1963–1973.

Broos N, Diergaarde L, Schoffelmeer AN, Pattij T, De Vries TJ (2012) Trait impulsive choice predicts resistance to extinction and propensity to relapse to cocaine seeking: a bidirectional investigation. Neuropsychopharmacology 37:1377–1386.

Buckholtz JW, Treadway MT, Cowan RL, Woodward ND, Li R, Ansari MS, Baldwin RM, Schwartzman AN, Shelby ES, Smith CE, Kessler RM, Zald DH (2010) Dopaminergic network differences in human impulsivity. Science 329:532.

Caprioli D, Jupp B, Hong YT, Sawiak SJ, Ferrari V, Wharton L, Williamson DJ, McNabb C, Berry D, Aigbirhio FI, Robbins TW, Fryer TD, Dalley JW (2015) Dissociable rate-dependent effects of oral methylphenidate on impulsivity and D2/3 receptor availability in the striatum. J Neurosci 35:3747–3755.

Caravaggio F, Fervaha G, Chung JK, Gerretsen P, Nakajima S, Plitman E, Iwata Y, Wilson A, Graff-Guerrero A (2016) Exploring personality traits related to dopamine D2/3 receptor availability in striatal subregions of humans. Eur Neuropsychopharmacol 26:644–652.

Cardinal RN, Pennicott DR, Sugathapala CL, Robbins TW, Everitt BJ (2001) Impulsive choice induced in rats by lesions of the nucleus accumbens core. Science 292:2499–2501.

Cheung TH, Cardinal RN (2005) Hippocampal lesions facilitate instrumental learning with delayed reinforcement but induce impulsive choice in rats. BMC Neurosci 6:36.

Christakou A, Brammer M, Rubia K (2011) Maturation of limbic corticostriatal activation and connectivity associated with developmental changes in temporal discounting. Neuroimage 54:1344–1354.

Costa Dias TG, Wilson VB, Bathula DR, Iyer SP, Mills KL, Thurlow BL, Stevens CA, Musser ED, Carpenter SD, Grayson DS, Mitchell SH, Nigg JT, Fair DA (2013) Reward circuit connectivity relates to delay discounting in children with attention-deficit/hyperactivity disorder. Eur Neuropsychopharmacol 23:33–45.

Dalley JW, Everitt BJ, Robbins TW (2011) Impulsivity, compulsivity, and top-down cognitive control. Neuron 69:680–694.

Dalley JW, Fryer TD, Brichard L, Robinson ES, Theobald DE, Lääne K, Peña Y, Murphy ER, Shah Y, Probst K, Abakumova I, Aigbirhio FI, Richards HK, Hong Y, Baron JC, Everitt BJ, Robbins TW (2007) Nucleus accumbens D2/3 receptors predict trait impulsivity and cocaine reinforcement. Science 315:1267–1270.

Dalley JW, Robbins TW (2017) Fractionating impulsivity: neuropsychiatric implications. Nat Rev Neurosci 18:158–171.

Davis FC, Knodt AR, Sporns O, Lahey BB, Zald DH, Brigidi BD, Hariri AR (2013) Impulsivity and the modular organization of resting-state neural networks. Cereb Cortex 23:1444–1452.

Dawe S, Loxton NJ (2004) The role of impulsivity in the development of substance use and eating disorders. Neurosci Biobehav Rev 28:343–351.

Galanti K, Gluck ME, Geliebter A (2007) Test meal intake in obese binge eaters in relation to impulsivity and compulsivity. Int J Eat Disord 40:727–732.

Genovese CR, Lazar NA, Nichols T (2002) Thresholding of statistical maps in functional neuroimaging using the false discovery rate. Neuroimage 15:870–878.

Ghahremani DG, Lee B, Robertson CL, Tabibnia G, Morgan AT, De Shetler N, Brown AK, Monterosso JR, Aron AR, Mandelkern MA, Poldrack RA, London ED (2012) Striatal dopamine D(2)/D(3) receptors mediate response inhibition and related activity in frontostriatal neural circuitry in humans. J Neurosci 32:7316–7324.

Gorges M, Müller HP, Lulé D, Pinkhardt EH, Ludolph AC, Kassubek J, LANDSCAPE Consortium (2015) To rise and to fall: functional connectivity in cognitively normal and cognitively impaired patients with parkinson's disease. Neurobiol Aging 36:1727–1735.

Gorges M, Müller HP, Lulé D, Pinkhardt EH, Ludolph AC, Kassubek J, LANDSCAPE Consortium (2016) The association between alterations of eye movement control and cerebral intrinsic functional connectivity in parkinson's disease. Brain Imaging Behav 10:79–91.

Gorges M, Roselli F, Müller HP, Ludolph AC, Rasche V, Kassubek J (2017) Functional connectivity mapping in the animal model: principles and applications of resting-state fmri. Front Neurol 8:200.

Isherwood SN, Robbins TW, Nicholson JR, Dalley JW, Pekcec A (2017) Selective and interactive effects of d2receptor antagonism and positive allosteric mglur4 modulation on waiting impulsivity. Neuropharmacology 123:249–260.

Jonckers E, Van Audekerke J, De Visscher G, Van der Linden A, Verhoye M (2011) Functional connectivity fmri of the rodent brain: comparison of functional connectivity networks in rat and mouse. Plos One 6:e18876.

Kilkenny C, Browne WJ, Cuthill IC, Emerson M, Altman DG (2012) Improving bioscience research reporting: the ARRIVE guidelines for reporting animal research. Osteoarthritis Cartilage 20:256–260.

Kohno M, Morales AM, Ghahremani DG, Hellemann G, London ED (2014) Risky decision making, prefrontal cortex, and mesocorticolimbic functional connectivity in methamphetamine dependence. JAMA Psychiatry 71:812–820.

Laird AR, Fox PM, Eickhoff SB, Turner JA, Ray KL, McKay DR, Glahn DC, Beckmann CF, Smith SM, Fox PT (2011) Behavioral interpretations of intrinsic connectivity networks. J Cogn Neurosci 23:4022–4037.

Lee B, London ED, Poldrack RA, Farahi J, Nacca A, Monterosso JR, Mumford JA, Bokarius AV, Dahlbom M, Mukherjee J, Bilder RM, Brody AL, Mandelkern MA (2009) Striatal dopamine d2/d3 receptor availability is reduced in methamphetamine dependence and is linked to impulsivity. J Neurosci 29:14734–14740.

Lipszyc J, Schachar R (2010) Inhibitory control and psychopathology: a meta-analysis of studies using the stop signal task. J Int Neuropsychol Soc 16:1064–1076.

London ED, Ernst M, Grant S, Bonson K, Weinstein A (2000) Orbitofrontal cortex and human drug abuse: functional imaging. Cereb Cortex 10:334–342.

London ED, Kohno M, Morales AM, Ballard ME (2015) Chronic methamphetamine abuse and corticostriatal deficits revealed by neuroimaging. Brain Res 1628:174–185.

Maier FC, Wehrl HF, Schmid AM, Mannheim JG, Wiehr S, Lerdkrai C, Calaminus C, Stahlschmidt A, Ye L, Burnet M, Stiller D, Sabri O, Reischl G, Staufenbiel M, Garaschuk O, Jucker M, Pichler BJ (2014) Longitudinal PET-MRI reveals β-amyloid deposition and rcbf dynamics and connects vascular amyloidosis to quantitative loss of perfusion. Nat Med 20:1485–1492.

Mobini S, Body S, Ho MY, Bradshaw CM, Szabadi E, Deakin JF, Anderson IM (2002) Effects of lesions of the orbitofrontal cortex on sensitivity to delayed and probabilistic reinforcement. Psychopharmacology (Berl) 160:290–298.

Moschak TM, Carelli RM (2017) Impulsive rats exhibit blunted dopamine release dynamics during a delay discounting task independent of cocaine history. eNeuro 4:doi: 10.1523/ENEURO.0119-17.2017.

Mukherjee J, Yang ZY, Das MK, Brown T (1995) Fluorinated benzamide neuroleptics–III. Development of (S)-N-[(1-allyl-2-pyrrolidinyl)methyl]-5-(3-[18F]fluoropropyl)-2, 3-dimethoxybenzamide as an improved dopamine D-2 receptor tracer. Nucl Med Biol 22:283–296.

Mukherjee J, Christian BT, Dunigan KA, Shi B, Narayanan TK, Satter M, Mantil J (2002) Brain imaging of 18F-fallypride in normal volunteers: blood analysis, distribution, test-retest

studies, and preliminary assessment of sensitivity to aging effects on dopamine D-2/D-3 receptors. Synapse 46:170–188.

Müller HP, Unrath A, Ludolph AC, Kassubek J (2007) Preservation of diffusion tensor properties during spatial normalization by use of tensor imaging and fibre tracking on a normal brain database. Phys Med Biol 52:N99–109.

Müller HP, Kassubek J, Vernikouskaya I, Ludolph AC, Stiller D, Rasche V (2013) Diffusion tensor magnetic resonance imaging of the brain in APP transgenic mice: a cohort study. Plos One 8:e67630.

Nederkoorn C, Braet C, Van Eijs Y, Tanghe A, Jansen A (2006) Why obese children cannot resist food: the role of impulsivity. Eat Behav 7:315–322.

Patros CH, Alderson RM, Kasper LJ, Tarle SJ, Lea SE, Hudec KL (2016) Choice-impulsivity in children and adolescents with attention-deficit/hyperactivity disorder (ADHD): a meta-analytic review. Clin Psychol Rev 43:162–174.

Plichta MM, Vasic N, Wolf RC, Lesch KP, Brummer D, Jacob C, Fallgatter AJ, Grön G (2009) Neural hyporesponsiveness and hyperresponsiveness during immediate and delayed reward processing in adult attention-deficit/hyperactivity disorder. Biol Psychiatry 65:7–14.

Pothuizen HH, Jongen-Rêlo AL, Feldon J, Yee BK (2005) Double dissociation of the effects of selective nucleus accumbens core and shell lesions on impulsive-choice behaviour and salience learning in rats. Eur J Neurosci 22:2605–2616.

Power JD, Barnes KA, Snyder AZ, Schlaggar BL, Petersen SE (2012) Spurious but systematic correlations in functional connectivity MRI networks arise from subject motion. Neuroimage 59:2142–2154.

Robbins TW, Gillan CM, Smith DG, de Wit S, Ersche KD (2012) Neurocognitive endophenotypes of impulsivity and compulsivity: towards dimensional psychiatry. Trends Cogn Sci 16:81–91.

Robertson CL, Ishibashi K, Mandelkern MA, Brown AK, Ghahremani DG, Sabb F, Bilder R, Cannon T, Borg J, London ED (2015) Striatal D1- and D2-type dopamine receptors are linked to motor response inhibition in human subjects. J Neurosci 35:5990–5997.

Rudebeck PH, Murray EA (2014) The orbitofrontal oracle: cortical mechanisms for the prediction and evaluation of specific behavioral outcomes. Neuron 84:1143–1156.

Rudebeck PH, Walton ME, Smyth AN, Bannerman DM, Rushworth MF (2006) Separate neural pathways process different decision costs. Nat Neurosci 9:1161–1168.

Sanefuji M, Craig M, Parlatini V, Mehta MA, Murphy DG, Catani M, Cerliani L, Thiebaut de Schotten M (2017) Double-dissociation between the mechanism leading to impulsivity and inattention in attention deficit hyperactivity disorder: a resting-state functional connectivity study. Cortex 86:290–302.

Schoenbaum G, Roesch MR, Stalnaker TA, Takahashi YK (2009) A new perspective on the role of the orbitofrontal cortex in adaptive behaviour. Nat Rev Neurosci 10:885–892.

Sforazzini F, Schwarz AJ, Galbusera A, Bifone A, Gozzi A (2014) Distributed BOLD and CBV-weighted resting-state networks in the mouse brain. Neuroimage 87:403–415.

Smith AJ, Becker S, Kapur S (2005) A computational model of the functional role of the ventral-striatal D2 receptor in the expression of previously acquired behaviors. Neural Comput 17:361–395.

Smith SM, Fox PT, Miller KL, Glahn DC, Fox PM, Mackay CE, Filippini N, Watkins KE, Toro R, Laird AR, Beckmann CF (2009) Correspondence of the brain's functional architecture during activation and rest. Proc Natl Acad Sci U S A 106:13040–13045.

Volkow ND, Wang GJ, Fowler JS, Telang F (2008) Overlapping neuronal circuits in addiction and obesity: evidence of systems pathology. Philos Trans R Soc Lond B Biol Sci 363:3191–3200.

Volkow ND, Wang GJ, Kollins SH, Wigal TL, Newcorn JH, Telang F, Fowler JS, Zhu W, Logan J, Ma Y, Pradhan K, Wong C, Swanson JM (2009) Evaluating dopamine reward pathway in ADHD: clinical implications. Jama 302:1084–1091.

Volkow ND, Wang GJ, Tomasi D, Kollins SH, Wigal TL, Newcorn JH, Telang FW, Fowler JS, Logan J, Wong CT, Swanson JM (2012) Methylphenidate-elicited dopamine increases in ventral striatum are associated with long-term symptom improvement in adults with attention deficit hyperactivity disorder. J Neurosci 32:841–849.

Wang GJ, Volkow ND, Thanos PK, Fowler JS (2004) Similarity between obesity and drug addiction as assessed by neurofunctional imaging: a concept review. J Addict Dis 23:39–53.

Winstanley CA, Theobald DE, Cardinal RN, Robbins TW (2004) Contrasting roles of basolateral amygdala and orbitofrontal cortex in impulsive choice. J Neurosci 24:4718–4722.

Zeeb FD, Floresco SB, Winstanley CA (2010) Contributions of the orbitofrontal cortex to impulsive choice: interactions with basal levels of impulsivity, dopamine signalling, and reward-related cues. Psychopharmacology (Berl) 211:87–98.

Zhan Y, Paolicelli RC, Sforazzini F, Weinhard L, Bolasco G, Pagani F, Vyssotski AL, Bifone A, Gozzi A, Ragozzino D, Gross CT (2014) Deficient neuron-microglia signaling results in impaired functional brain connectivity and social behavior. Nat Neurosci 17:400–406.